Asian Journal of Chemistry; Vol. 26, No. 15 (2014), 4887-4892

ASIAN JOURNAL OF CHEMISTRY

http://dx.doi.org/10.14233/ajchem.2014.16512

Ratiometric Nanosensor for Visual Detection of Copper Ions

SHENGDA QI, CUILING REN*, YANPING CHANG, HONGLI CHEN, YONGLEI CHEN, XINGGUO CHEN and YUJIE XIE

Department of Chemistry, Lanzhou University, Lanzhou 730000, P.R. China

*Corresponding author: Fax: +86 931 8912582; Tel: +86 931 8912763; E-mail: rencl@lzu.edu.cn

Received: 10 October 2013; *Accepted*: 14 March 2014; *Published online*: 16 July 2014; AJC-15593

In this paper, a new ratiometric fluorescent nanosensor was synthesized simply and economically and applied for Cu^{2+} detection in water samples. This nanosensor was a type of dual-emission quantum dots which was composed silica coated red CdTe quantum dots and glutathione modified green CdTe quantum dots. The probe exhibits a dynamic response range for Cu^{2+} from 6.7×10^{-8} to 8×10^{-7} mol L^{-1} with a detection limit of 2.5×10^{-8} mol L^{-1}. Other alkali, alkaline earth and transitional metal ions including K^+, Na^+, Mg^{2+}, Zn^{2+}, Pb^{2+}, Ni^{2+}, Cr^{3+} and Fe^{3+} had no significant interferences on Cu^{2+} determination. Binding Cu^{2+} to the nanosensor make the colour of the solution change from green to orange under UV light irradiation, which illustrates that this new sensor can realize visually detection of Cu^{2+}.

Keywords: Ratiometric fluorescent nanosensor, Dual-emission quantum dots, Copper ion.

INTRODUCTION

Copper ion is an important transition metal ion in the human body, which plays important roles in various biological processes in organisms ranging from bacteria to mammals[1-4]. But high concentration of copper ion can cause oxidative stress and disorders correlated with neurodegenerative diseases, including Alzheimer's disease, prion disease, Parkinson's diseases and Amyotrophic Lateral Sclerosis[5]. Therefore it is important to accurately determine the concentration of Cu^{2+}. Numerous methods have been proposed for the detection of copper ion, including atomic absorption spectrometry, inductively coupled plasma mass spectroscopy and voltammetry[6-8]. These methods offer good limits of detection and wide working concentration ranges. However, these methods may require the use of sophisticated and relatively costly apparatus.

Chemical sensors, which could overcome these disadvantages, are becoming more and more important for monitoring metal ion. The most frequently used chemical sensor for Cu^{2+} detection is organic dye[9,10], gold nanomaterials[11,12] and ratiometric sensor[13-16]. Among these materials, ratiometric sensors have attracted more and more attention in recent years. Ratiometric method is an alternative to classical detection method which based on intensity measurements. It is considered to be more efficient because it is better resistance to background and instrumental fluctuations. Furthermore, ratiometric method is based on the intensity ratios at two different wavelengths which make it very useful in eliminating most or all ambiguities by self-calibration of two emission bands. Additionally, ratiometric fluorescent detection can make the detection process visible[17-20]. This method has been applied in biochemistry, metal ion recognition and pH, *etc.*[21-27].

The unique properties of quantum dots (QDs, semiconductor nanoparticles), including wide excitation and narrow emission wavelengths, resistance to photobleaching, along with high quantum yield in aqueous solutions, make dual emission quantum dots an alternative to dual emission dye or organic molecules. Up to now, few quantum dot-based ratiometric sensors have been reported [28-32]. Zhang *et al.*[31] have prepared a ratiometric fluorescent sensor for the detection of trace trinitrotoluene explosives. Their method was simple and efficient. Yao *et al.*[32] designed a ratiometric fluorescence probe by hybridizing dual-emission quantum dots and demonstrated its efficiency for on-site visual determination of copper ions. Compared this synthetic probe method, our method is simple and save time.

This paper reports a dual-emission fluorescent nanosensor for Cu^{2+} detection based on dual-emissions quantum dots. The synthetic procedure is illustrated in **Scheme-I**. Silica coated red emission quantum dots was used as core and GSH modified green emission quantum dots was used as shell. The photoluminescent spectra of the core, shell and dual emission sensor were also presented in **Scheme-I**, which proved the new prepared sensor possess two distinguish emission peak at 520 nm and 604 nm. Binding Cu^{2+} to the nanosensor can makes it change from green to orange under UV light irradiation. So it can be used to detect Cu^{2+} visually. The synthesis and charac-

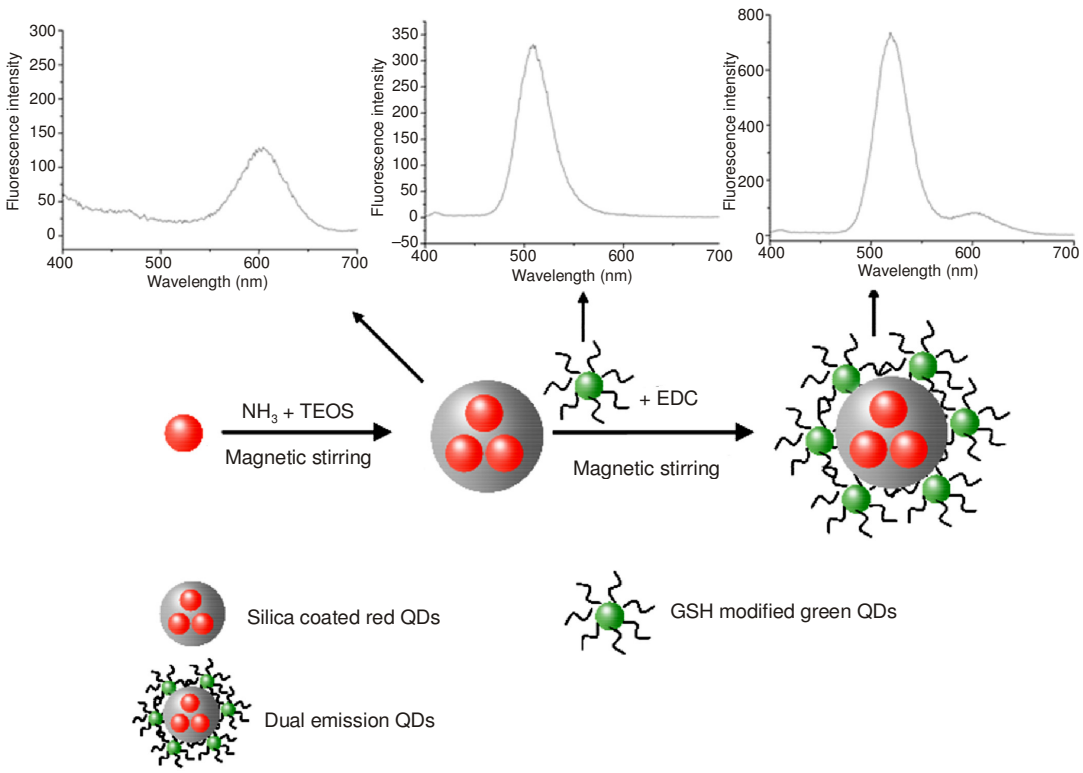

Scheme-1: Illustration of the synthetic process of dual emission nanosensor and the corresponding emission spectra of red quantum dots, green quantum dots (QDs) and the dual emission nanosensor

terization of this new material, including particle size, morphology and fluorescent properties were presented.

EXPERIMENTAL

Cadmium chloride ($CdCl_2·2.5H_2O$) and sodium borohydride ($NaBH_4$) were purchased from Shanghai Chemical Reagents Factory, China. Te powder was purchased from Sinopharm Chemical Reagent Co., Ltd. Thioglycolic acid (TGA, 90 %) was obtained from Tianjin Guangfu Fine Chemical Research Institute, China. 1-[3-(Dimethylamino)-propyl]-3-ethylcarbodiimide hydrochloride (EDC) and glutathione were bought from Sheng Gong biological engineering Co., Ltd (Shanghai, China). Tetraethylorthosilicate (TEOS) was obtained from Tianjin chemical reagent company, China. Mercaptopropyltrimethoxysilane was purchased from Fluka chemical company. 3-aminopropyltriethoxysilane (APTES) was commercially available from J&K Scientific Ltd. (Beijing, China). All chemicals were of analytical grade and used as received without further purification. Deionized water was used throughout the work.

All fluorescence spectra were measured on a RF-5301PC fluorescence spectrophotometer (Shimadzu, Japan). pH measurements were performed on pHs-3C (Leici Analytical Instrument Factory, Shanghai, China). UV light was from a low intensity UV lamp (365 nm, WFH-203, Shanghai Jingke Industrial Co. Ltd.). All transmission electron micrographs were carried out on a Tecnai TF20 transmission electron microscope (TEM) (FEI, USA).

Preparation and surface modification of silica coated red CdTe quantum dots: 114.2 g $CdCl_2·2.5H_2O$, 63 mL H_2O and 105 µL thioglycolic acid were added into a three-necked bottle and the pH was adjusted to 9 by 1.25 mol L^{-1} NaOH under nitrogen protection. NaHTe was synthesized using 31.9 mg Te powder, 50 mg $NaBH_4$ and 5 mL H_2O. Then the two solutions were mixed under nitrogen protection for 20 min followed by refluxing at 90 °C for 14 h.

Then the prepared red CdTe quantum dots (40 mL) were mixed with 80 mL ethanol and 40 µL mercaptopropyltrimethoxysilane. After the mixture stirred for 6 h at room temperature, 2 mL TEOS and 2 mL ammonia was added and stirred for 12 h at room temperature. After that, 100 µL APTES was added and reacted for 12 h in order to modify the surface of the particles with amino group. After centrifugation, the obtained red quantum dots were washed with deionized water and ethanol. Finally, the product was vacuum dried at 40 °C.

Preparation of glutathione modified green CdTe quantum dots: Glutathione (GSH)-capped CdTe quantum dots were synthesized following a method reported by Ying *et al.*[33] with minor modification. Typically, 57.1 mg $CdCl_2·2.5H_2O$ and 76.3 mg glutathione were mixed in 50 mL H_2O and the pH of the mixture was adjusted to 8 by using 1.25 mol L^{-1} NaOH under magnetic stirring. Under pure N_2 protection, fresh NaHTe which was prepared by 8 mg Te, 15.9 mg $NaBH_4$ and 5 mL H_2O was injected and the mixture was heated to reflux for 1 h under N_2 protection.

Preparation of dual-emission quantum dots: 5 mg red quantum dots doped silica nanoparticles and 0.5 mL glutathione modified green quantum dots solution were added to 10 mL NaH_2PO_4-Na_2HPO_4 buffer (pH = 9, 0.05 mol L^{-1}), then 2 mg EDC was added and the reaction system was continued for 2 h.

Procedures for Cu^{2+} Sensing: A standard stock solution of Cu^{2+} (4×10^{-5} mol L^{-1}) was prepared by dissolving an

appropriate amount of $CuSO_4.5H_2O$ in water. Stock solutions of other metal ions were prepared in water with a similar procedure.

The 1 cm quartz cell was first filled with 3 mL NaH_2PO_4-Na_2HPO_4 buffer solution (pH = 9, 0.05 mol L^{-1}) and 300 µL the prepared dual-emission quantum dots solution. Then, the fluorescent spectra were recorded under 360 nm excitation. The influence of pH on the fluorescent intensity of this new sensor was conducted under the same procedure except changing the pH value of the buffer solution (6, 7, 8, 9 and 10). After the fluorescent intensity recorded, 50 µL 4×10^{-5} mol L^{-1} Cu^{2+} solutions were added and the fluorescent intensity were also recorded. The stability of this new sensor was studied by measuring its fluorescent intensity in the range of 0-90 min. The optimum detection time for Cu^{2+} was studied by measuring the photoluminescence signal of the new sensor solution after the addition of 50 µL Cu^{2+} solutions in the time range of 0-8 min with 1 min intervals. Interference of other metallic ions on determination of Cu^{2+} was conducted with the same concentration (4×10^{-5} mol L^{-1}, 50 µL) and procedure. In order to obtain the calibration curves, different volume (5, 10, 20, 30, 40, 50, 60, 70 and 80 µL) of Cu^{2+} solution were added to the sensor solution and recorded their emission signal intensity.

RESULTS AND DISCUSSION

TEM images of prepared dual-emission quantum dots: The morphology and size of the prepared silica coated red quantum dots and dual emission nanosensor was characterized by TEM. Fig. 1a showed the morphology of the prepared silica coated red quantum dots is spherical and their sizes are about 150 nm. After they conjugated with GSH modified green quantum dots (Fig. 1b), their particles shape and sizes are not much changed, but the particles were aggregated at some extent.

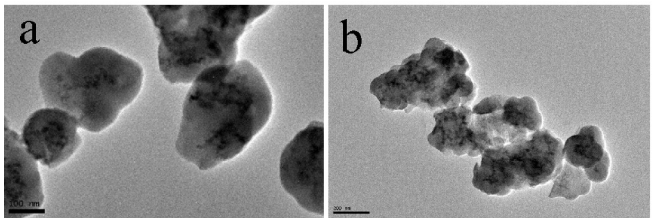

Fig. 1. TEM images of the prepared silica coated red quantum dots (QDs) (a) and dual-emission QDs (b)

Spectral characteristics of the prepared dual-emission quantum dots: The optical property of the prepared dual-emission quantum dots and its response to Cu^{2+} were characterized by fluorescence spectrophotometer and UV light irradiation, the results are shown in Fig. 2. It showed that the prepared new nanosensor solution has two well-resolved emission peaks at 520 and 604 nm under a single wavelength excitation and the solution is green under UV irradiation. After adding 50 µL Cu^{2+} solution, the emission intensity at 520 nm

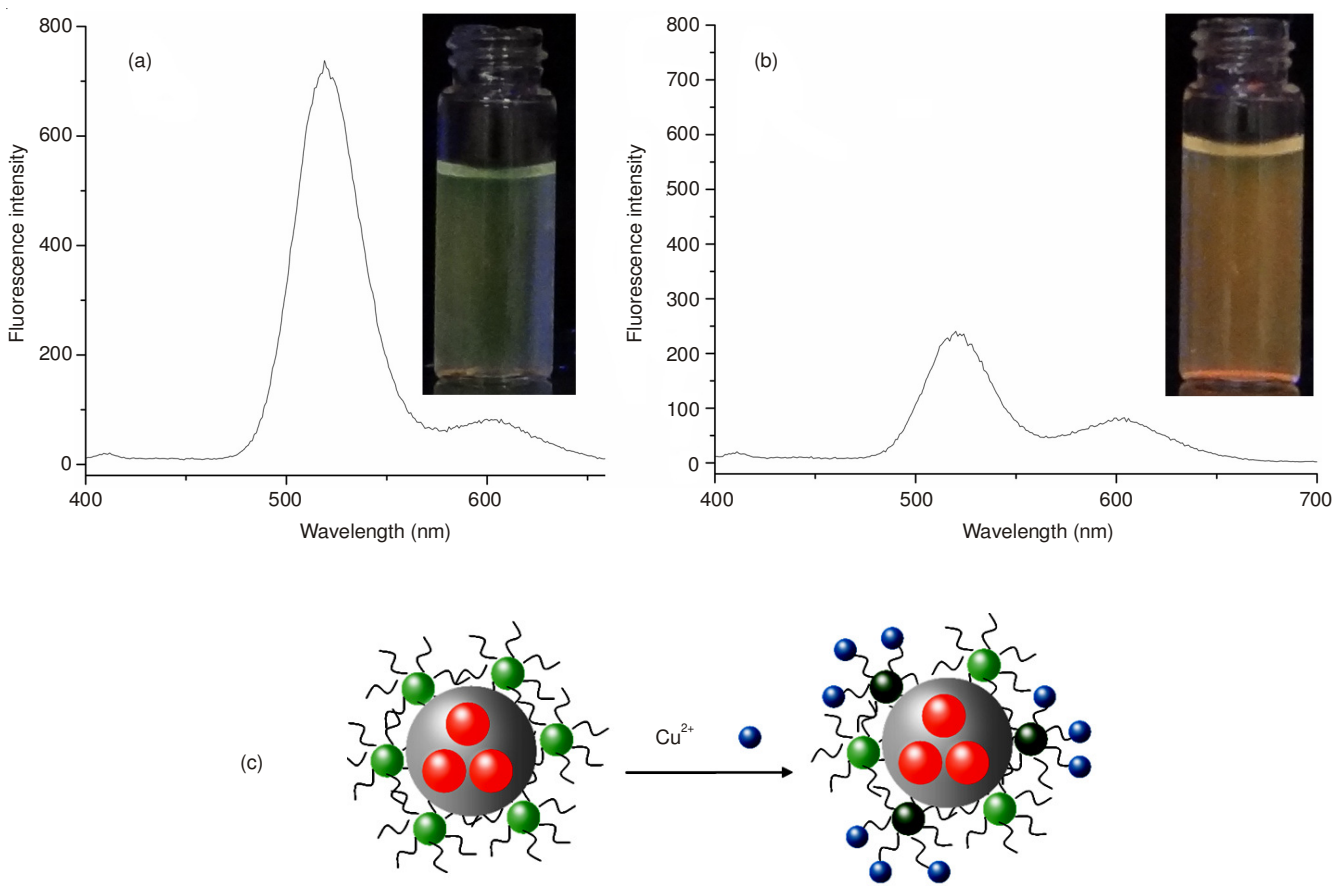

Fig. 2. Fluorescence emission spectra and photograph of the prepared dual emission nanosensor (a) and its response to Cu^{2+} (b) under UV light irradiation and their detection mechanism (c)

decreased evidently (Fig. 2b), whereas the emission intensity at 604 nm from the encapsulated red quantum dots remains constant. It proved that the fluorescence intensity of the red quantum dots of the dual-emission quantum dots was not influenced by the Cu^{2+} ions, but the outer glutathione modified quantum dots can response sensitively to Cu^{2+} ions. The intensity ratio variations of the two emission wavelengths make the colour of the prepared dual emission quantum dots changed from green to orange, facilitating the detection of Cu^{2+} by naked eyes.

The mechanism is shown in Fig. 2c. Glutathione (GSH) is a tripeptide composed of glutamic acid, cysteine and glycine. The thiol groups of cysteine can be used as capping agent to prepare highly fluorescent GSH-capped quantum dots (GSH-QDs). Each GSH molecule also contains one amine and two carboxylate groups, so GSH-QDs can be used as selective fluorescent probes to heavy metal ions[34]. In this work, glutathione modified green quantum dots whose fluorescent intensity could be quenched by Cu^{2+}, but the silica coated red quantum dots which was insensitive to the outer environment were used as core.

Optimization of detection conditions: In order to achieve an optimal detection performance, we carefully optimized the assay conditions, including the pH value of the NaH_2PO_4-Na_2HPO_4 buffer, the stability of the sensor and the signal changing with time after they reacted with Cu^{2+}.

Effect of buffer pH: The influence of the pH of NaH_2PO_4-Na_2HPO_4 buffer on the performance of the dual emission quantum dots was carried out in the range of pH from 7 to 10. The plots of log (I_{520}/I_{604}) and Q_p *versus* pH were shown in Fig. 3, where I_{520}/I_{604} was the initial fluorescence intensity ratio and Q_p was the quenching percentage after the addition of Cu^{2+} calculated by the following equation:

$$Qp = \frac{(I_{520}/I_{604})_{\text{without } Cu^{2+}} - (I_{520}/I_{604})_{\text{with } Cu^{2+}}}{(I_{520}/I_{604})_{\text{without } Cu^{2+}}} \times 100\ \%$$

As shown in Fig. 3, I_{520}/I_{604} enhanced with increasing pH from 7 to 9 whereas Q_p reduced with the buffer pH increasing. Theoretically, a higher value of I_{520}/I_{604} implied a wider detection range of Cu^{2+} and a large Q_p might improved the detection sensitivity. In order to achieve wider detection range and higher detection sensitivity, 9 was chosen as the optimum pH value for the detection of Cu^{2+}.

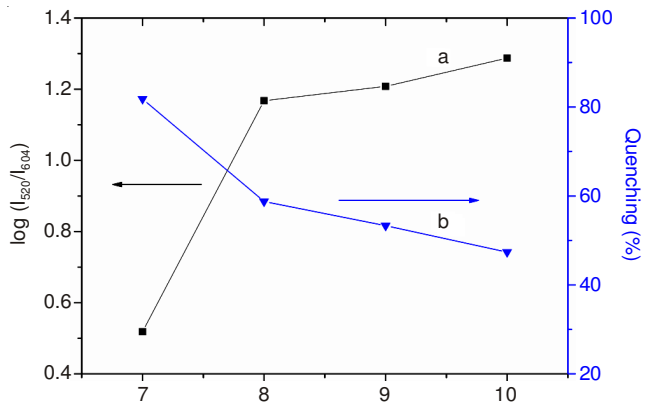

Fig. 3. Effect of NaH_2PO_4-Na_2HPO_4 buffer pH on (■) fluorescence intensity ratio (I_{520}/I_{604}) of dual emission quantum dots and (▼) and quenching percentage of the prepared dual emission quantum dots after the addition of Cu^{2+}, the concentration of Cu^{2+} is 6.7×10^{-7} mol L^{-1}

Stabilization of fluorescence intensity: In order to investigate the stabilization of the prepared dual-emission quantum dots in NaH_2PO_4-Na_2HPO_4 buffer solution, the fluorescence signal was recorded during 90 min (as depicted in Fig. 4). It was indicated that no significant changes in fluorescent intensity were observed with time flowing. It showed that the fluorescence signal of the prepared dual emission quantum dots is stable during the analytical measurements procedure.

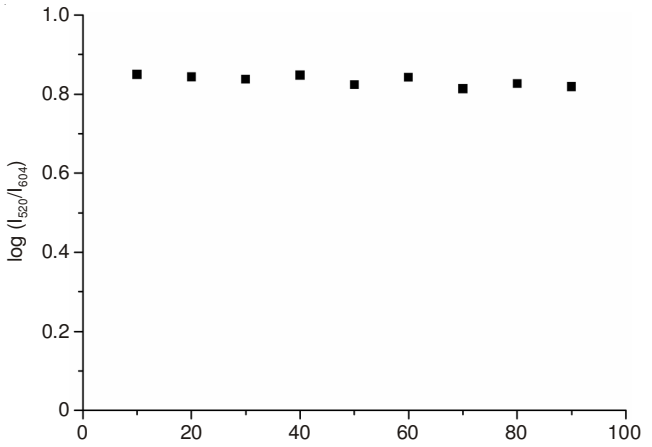

Fig. 4. Time course of the fluorescence intensity ratio (I_{520}/I_{604}) of dual emission quantum dots in NaH_2PO_4-Na_2HPO_4 buffer solution (50 mmol L^{-1}, pH 9)

Optimization of detection time for Cu^{2+}: As the fluorescent signal of the prepared dual emission quantum dots can be quenched by Cu^{2+}, so it was important to study their signal evolution with time after the addition of Cu^{2+}. With all the other experimental conditions fixed, the change of the fluorescent signal after the addition of 50 µL Cu^{2+} solutions was recorded in 1-8 min. As shown in Fig. 5, log (I_{520}/I_{604}) decreased significantly from 0.82 to 0.3 after the addition of Cu^{2+} in 1 min. Then log (I_{520}/I_{604}) decreased slightly during the period of 2-4 min and kept stable after 4 min. So 5 min was chosen as the optimum detection time after the addition of Cu^{2+}.

To sum up, the optimum detection conditions were as follows: the pH of the buffer was 9, the detect time was 5 min after the addition of Cu^{2+}.

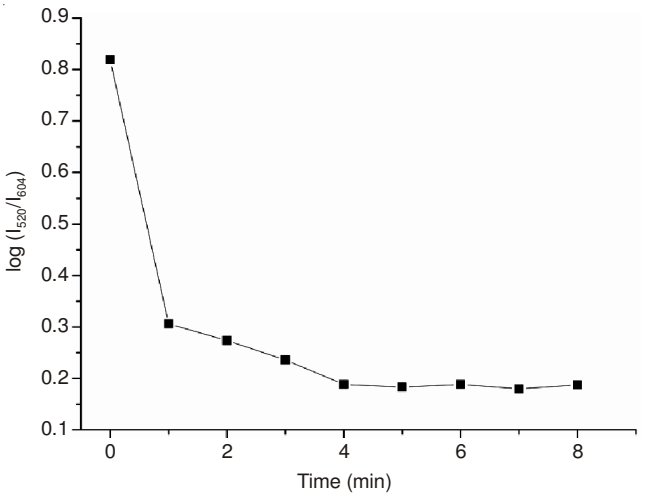

Fig. 5. Fluorescence intensity ratio (I_{520}/I_{604}) variations of the prepared dual-emission nanosensors with time in the presence of Cu^{2+}

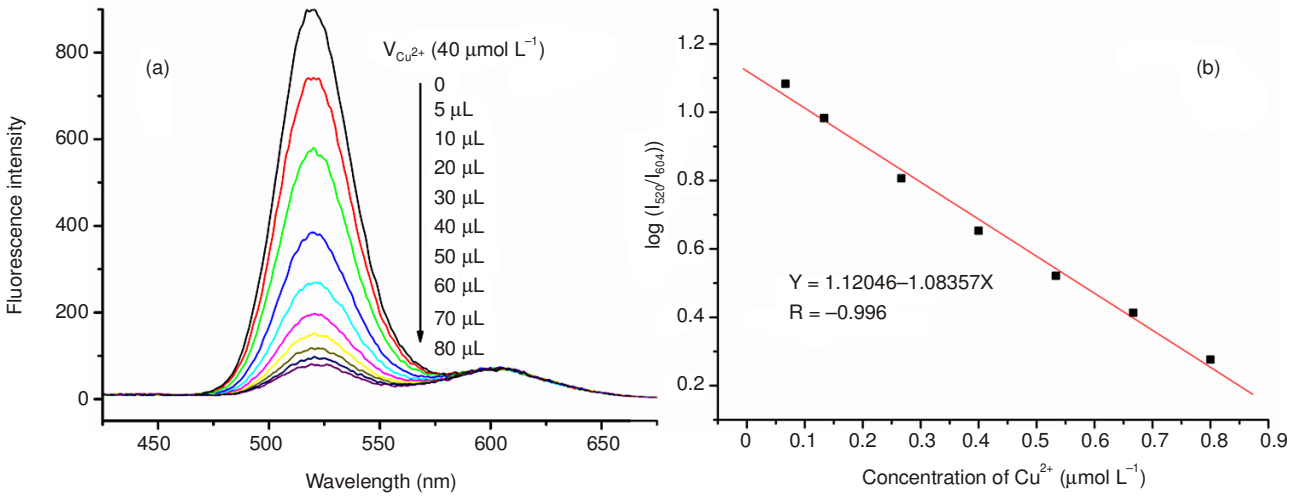

Fig. 6. Fluorescence emission spectra of the ratiometric nanosensor solution in the presence of different amount Cu^{2+} (a) and calibration curves (b)

Method validation: Fluorescence spectra of the dual emission nanosensor solution in the presence of different amount of Cu^{2+} and calibration curves were investigated under the optimum conditions and the results are shown in Fig. 6. Fig. 6a showed that the emission intensity at 520 nm decreases linearly with the concentration of Cu^{2+}. Fig. 6b displays the fluorescence spectra of the ratiometric sensor as a function of the concentration of Cu^{2+}, a good linear relationship (R = 0.996) was found between the logarithm of (I_{520}/I_{604}) and the concentration of Cu^{2+} over the range from 6.7×10^{-8}-8×10^{-7} mol L^{-1}. The detection limit is calculated to be 2.5×10^{-8} mol L^{-1}.

Fig. 7 displayed the photograph of GSH-modified CdTe quantum dots (a) and the prepared dual emission quantum dots (b) in the presence of different volume of Cu^{2+} standard solutions under the optimum conditions. It is obvious that the colour of the GSH-modified CdTe quantum dots is green under the UV light irradiation and the colour shallowed by increasing the Cu^{2+} concentration. However, the decrease of the green emission of the dual emission quantum dots cause the colour of the prepared dual emission quantum dots gradually changed from green to red, facilitating the detection of Cu^{2+} by naked eyes.

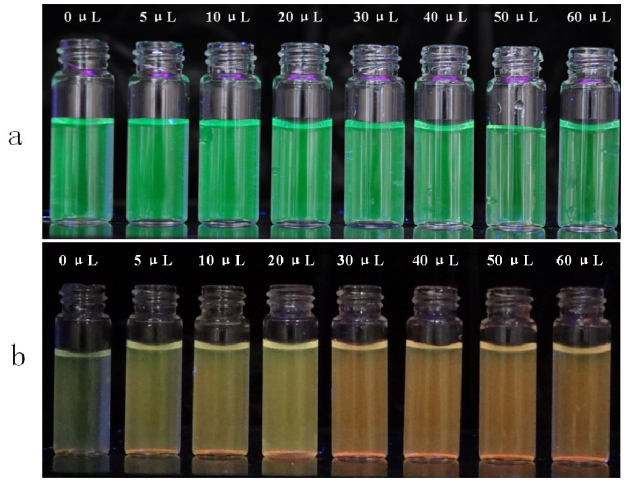

Fig. 7. Photograph GSH-modified CdTe quantum dots (a) and the prepared dual emission quantum dots (b) in the presence of different volume of Cu^{2+} under UV irradiation

Interference of other metallic ions in determination of Cu^{2+}: In order to investigate the selectivity of the dual-emission nanosensor for the determination of Cu^{2+}, it is important to evaluate the interference effect of some common foreign ions. Concentrations of all ions tested in the experiment were the same as that of the Cu^{2+} ion and the results was shown in Fig. 8. The fluorescence intensity of the prepared new sensor was quenched to different extent by Cu^{2+}, Ni^{2+}, Zn^{2+}, Mg^{2+}, Cr^{3+}, Pb^{2+}, Fe^{3+}, K^{+} and Na^{+} ions in the buffer solution. The result shows that Zn^{2+}, Mg^{2+}, Cr^{3+}, Pb^{2+}, Fe^{3+}, K^{+} and Na^{+} did not interfere the determination of Cu^{2+}. The luminescence intensity of the dual emission nanosensor is minimally affected by Ni^{2+}. As reported by the previous studies, Cu^{2+} detection is known to be interfered by Ni^{2+} because both ions form complexes with nitrogen containing functional group[35].

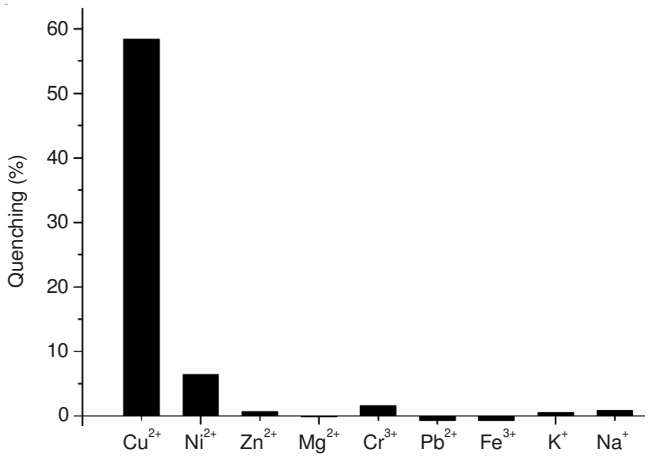

Fig. 8. Selectivity of the dual-emission nanosensor for Cu^{2+} over other metallic ions, the concentrations of the detected cations were all 6.7×10^{-8} μmol L^{-1}

Applications: In order to further explore the practicability of the proposed method, it was applied for detecting Cu^{2+} in tap water. The determination results were shown in Table-1. Additionally, recoveries were investigated by adding a known amount of Cu^{2+} to the water samples to demonstrate the accuracy of the method. The result showed that the recoveries for Cu^{2+} at three spiked levels ranging from 94 to 105 %. Good recovery for Cu^{2+} suggested that this method was largely free

TABLE-1
DETERMINATION RESULTS OF Cu^{2+} IONS IN WATER SAMPLE

Tap water sample	Spiked Cu^{2+} concentrations in tap water (mol L^{-1})	Detection amount (mol L^{-1})	RSD (n = 9) (%)	Recovery (%)
1	6.67×10^{-8}	6.40×10^{-8}	6.8	96
2	13.3×10^{-8}	14.0×10^{-8}	5.4	105
3	20.0×10^{-8}	18.9×10^{-8}	0.9	94

from the sample matrix effect of the water. For nine replicate measurements, the standard deviation of a solution containing 6.67×10^{-8}, 13.3×10^{-8} and 20×10^{-8} mol L^{-1} Cu^{2+} is 6.8, 5.4 and 0.9 %, which indicated a good reproducibility of the method.

Conclusion

A new nanosensor for detecting copper ions based on dual-emission quantum dots was prepared and characterized. The experimental results indicated that this new prepared dual-emission nanosensor can be applied to visually detect copper ions in water samples and the detection limit is 2.5×10^{-8} mol L^{-1}. This method may be useful for further research and practical applications of the novel dual emission nanosensor in the detection of other toxic materials.

ACKNOWLEDGEMENTS

This work was kindly supported by the National Natural Science Foundation of China (Nos. 21005035, 21207057 and J1103307), the Fundamental Research Funds for the Central Universities (Nos. lzujbky-2012-78 and lzujbky-2013-196), the basic scientific research business expenses of the central university and Open Project of Key Laboratory for Magnetism and Magnetic Materials of the Ministry of Education, Lanzhou University (No. LZUMMM2012004).

REFERENCES

1. L.M. Gaetke and C.K. Chow, *Toxicology*, **189**, 147 (2003).
2. X.B. Zhang, J. Peng, C.L. He, G.L. Shen and R.Q. Yu, *Anal. Chim. Acta*, **567**, 189 (2006).
3. E.L. Que, D.W. Domaille and C.J. Chang, *Chem. Rev*., **108**, 1517 (2008).
4. R. Uauy, M. Olivares and M. Gonzalez, *Am. J. Clin. Nutr*., **67**, 952S (1998).
5. E. Gaggelli, H. Kozlowski, D. Valensin and G. Valensin, *Chem. Rev*., **106**, 1995 (2006).
6. H. Faghihian, A. Hajishabani, S. Dadfarnia and H. Zamani, *Int. J. Environ. Anal. Chem*., **89**, 223 (2009).
7. D. Chen, B. Hu and C. Huang, *Talanta*, **78**, 491 (2009).
8. M.A. Nolan and S.P. Kounaves, *Anal. Chem*., **71**, 3567 (1999).
9. S. Khatua, S.H. Choi, J. Lee, J.O. Huh, Y. Do and D.G. Churchill, *Inorg. Chem*., **48**, 1799 (2009).
10. M. Royzen, Z. Dai and J.W. Canary, *J. Am. Chem. Soc*., **127**, 1612 (2005).
11. X. Xu, W.L. Daniel, W. Wei and C.A. Mirkin, *Small*, **6**, 623 (2010).
12. J.M. Liu, H.F. Wang and X.P. Yan, *Analyst*, **136**, 3904 (2011).
13. C. Zong, K. Ai, G. Zhang, H. Li and L. Lu, *Anal. Chem*., **83**, 3126 (2011).
14. K. Kaur and S. Kumar, *Dalton Trans*., **40**, 2451 (2011).
15. S. Goswami, D. Sen and N.K. Das, *Org. Lett*., **12**, 856 (2010).
16. Z. Xu, J. Yoon and D.R. Spring, *Chem. Commun.*, **46**, 2563 (2010).
17. X. Lv, J. Liu, Y. Liu, Y. Zhao, M. Chen, P. Wang and W. Guo, *Org. Biomol. Chem*., **9**, 4954 (2011).
18. F.J. Huo, J. Su, Y.Q. Sun, C.X. Yin, H.B. Tong and Z.X. Nie, *Dyes Pigments*, **86**, 50 (2010).
19. Y. Bao, B. Liu, H. Wang, J. Tian and R. Bai, *Chem. Commun.*, **47**, 3957 (2011).
20. Y.B. Ruan, C. Li, J. Tang and J. Xie, *Chem. Commun.*, **46**, 9220 (2010).
21. Q. Dai, W. Liu, X. Zhuang, J. Wu, H. Zhang and P. Wang, *Anal. Chem*., **83**, 6559 (2011).
22. G.J. Kim, K. Lee, H. Kwon and H.J. Kim, *Org. Lett*., **13**, 2799 (2011).
23. H. Zhu, W. Zhang, K. Zhang and S. Wang, *Nanotechnology*, **23**, 315502 (2012).
24. B. Zhu, C. Gao, Y. Zhao, C. Liu, Y. Li, Q. Wei, Z. Ma, B. Du and X. Zhang, *Chem. Commun.*, **47**, 8656 (2011).
25. Z.X. Han, X.B. Zhang, Z. Li, Y.J. Gong, X.Y. Wu, Z. Jin, C.M. He, L.X. Jian, J. Zhang, G.L. Shen and R.Q. Yu, *Anal. Chem*., **82**, 3108 (2010).
26. Z. Liu, C. Zhang, W. He, Z. Yang, X. Gao and Z. Guo, *Chem. Commun.*, **46**, 6138 (2010).
27. Z. Xu, K.H. Baek, H.N. Kim, J. Cui, X. Qian, D.R. Spring, I. Shin and J. Yoon, *J. Am. Chem. Soc*., **132**, 601 (2010).
28. T. Jin, A. Sasaki, M. Kinjo and J. Miyazaki, *Chem. Commun.*, **46**, 2408 (2010).
29. K. Paek, S. Chung, C.H. Cho and B.J. Kim, *Chem. Commun.*, **47**, 10272 (2011).
30. F. Ye, C. Wu, Y. Jin, Y.H. Chan, X. Zhang and D.T. Chiu, *J. Am. Chem. Soc*., **133**, 8146 (2011).
31. K. Zhang, H. Zhou, Q. Mei, S. Wang, G. Guan, R. Liu, J. Zhang and Z. Zhang, *J. Am. Chem. Soc*., **133**, 8424 (2011).
32. J. Yao, K. Zhang, H. Zhu, F. Ma, M. Sun, H. Yu, J. Sun and S. Wang, *Anal. Chem*., **85**, 6461 (2013).
33. Y. Zheng, S. Gao and J.Y. Ying, *Adv. Mater*., **19**, 376 (2007).
34. Y. Zheng, Z. Yang, Y. Li and J.Y. Ying, *Adv. Mater*., **20**, 3410 (2008).
35. T. Kang, S. Hong, J. Moon, S. Oh and J. Yi, *Chem. Commun.*, **41**, 3721 (2005).